Chapter - III

CHARACTERIZATION OF FERRITES

3.0 Introduction

Part A : X- ray diffraction

3.A.1 X-ray diffraction principle

3.A.2 Powder method

3.A.3 Experimental

3.A.4 Results and discussion

Part B : IR absorption

3.B.1 Experimental

3.B.2 Results and discussion

References

3.0 Introduction

Ferrites are characterized by chemical analysis, mass spectrum analysis, x-ray diffraction, neutron diffraction, saturation magnetization etc.

The phenomenon of x-ray diffraction by crystal was experimentally demonstrated by Laue in 1912. After successful analysis of Laue's experiments, Bragg [1] put forth his famous equation as $2d\sin\theta = n\lambda$. X-ray diffraction method developed by Bertaut [2], waren and Aberbach [3]. It is the well estabblished tool of crystallography.

Several investigators [4-10] calculated the lattice constant by using x-ray diffraction studies. P. Ravindranathan and K.C. Patil [11] have confirmed the formation of ultrafine Ni-Zn ferrites prepared by thermal decomposition precursors using XRD studies. They have observed fine particle nature of the ferrites. They have also reported that the average crystalline sizes of $Ni_xZn_{1-x}Fe_2O_4$ calculated from x-ray line broadening are found to be in the range of 10 to 40 nm.

H. Yamaura et al [12] carried out x-ray analysis of nickel ferrites and showed that, the sample fired at fairly low temperature have many crystal imperfections such as lattice strain and lattice defects. He attributed that the crystal imperfections decreased with increasing firing temperature and vanished at about 800 °C.

Kulkarni et al [13] have prepared magnesium ferrites by wet and ceramic method. On the basis of x-ray analysis, they have reported that the

wet prepared and ceramic prepared samples possessed single spinel phase. They also observed that x-ray diffraction lines were slightly broad for the wet prepared ferrites because of the fine particle size effect.

Ferrites can also be characterized by IR studies. Infrared spectra gives information about molecular structure, molecular behaviour and the identification of unknown chemical substances and mixture [14]. The vibrational, electronic and magnetic dipole spectra can gives information about the position and valancies of the ions in the crystal lattices. In the infrared region, the molecular vibrations gives rise to two absorption bands in the ferrites, which helps to compute the vibrational energy of the molecules [15].

Waldron [15] studied the infrared spectra of different ferrites in the frequency range 280 to 4000 cm^{-1}. He has shown that, two absorption occurs below 1000cm^{-1}. Jolsulu and Sobhandri [16] have noticed four fundamental active modes of vibrations for Co-Zn ferrites. They observed that the intensities of ν_3 and ν_4 bands increases with cobalt concentration.

Reddy and Salagram [17] have observed two prominent bands and two weak bands in the IR spectra of Mn-Mg ferrites. The prominent band ν_1 andν_2 are assigned to tetrahedral and octahedral metal oxygen complexes respectively. The band ν_3 is due to the octahedral divalent metal ion oxygen complex. For the lowest frequency band ν_4, the position and intensity

increases with Mg^{2+} content and is due to the lattice vibration in mixed ferrites.

With the help of infrared and Mossbauer spectra, Potakova [18] has confirmed the presence of Fe^{2+} on tetrahedral and octahedral sites in the $Ni_{1-x-y}Fe_x^{2+}Zn_yFe_2^{3+}O_4$.

Part A : X- ray diffraction

3.A.1 X-ray diffraction principle

The diffraction of x-rays by crystal is only possible when Bragg's condition is satisfied.

We have Bragg's condition

$$2d\sin\theta = n\lambda \qquad .....3.1$$

where n - integer number

d- interplaner distance

θ - glancing angle

λ - Wavelength of monochromatic x-ray

In most of the cases, the first order diffraction is used, then Bragg's law takes the form

$$\lambda = 2d_{hkl}\sin\theta_{hkl} \qquad ....3.2$$

By varying the wavelength(λ) or glancing angle θ, the crystal structure can be studied.

There are three important methods of x- ray diffraction based on the variation of wavelength (λ) and glancing angle (θ).

1) Laue method

2) Rotating crystal method

3) Powder method

The powder x-ray diffraction method usually used in ferrites.

3.A.2 Powder method

This method was first developed by Debye and Scherrer [19] in Germany and indenpendtly by Hull [20] in America. The essential features of diffractometer are shown in Fig. 3.1

In this method, the wavelength (λ) is fixed and specimen is rotated. The x-rays emiited from socurce 's' are initially made monochromatic by passing them through the appropriate filter. This monochromatic beam is then suitably collimated by slit A and allowed to fall on the powder specimen C, kept at the centre on the table T. The table is capable of rotating about an axis passing through O. The incident monochromatic beam was diffracted by the specimen to form a convergent diffracted beam. The convergent beam on passing through slit B focuses at F and then enetres in the counter G. The recieving slit and counter are supported on the carriage E, which may be rotated about the axis O. The angular position of counter may be read on the graduated sacle K. The carriage and table are mechanically coupled in such a

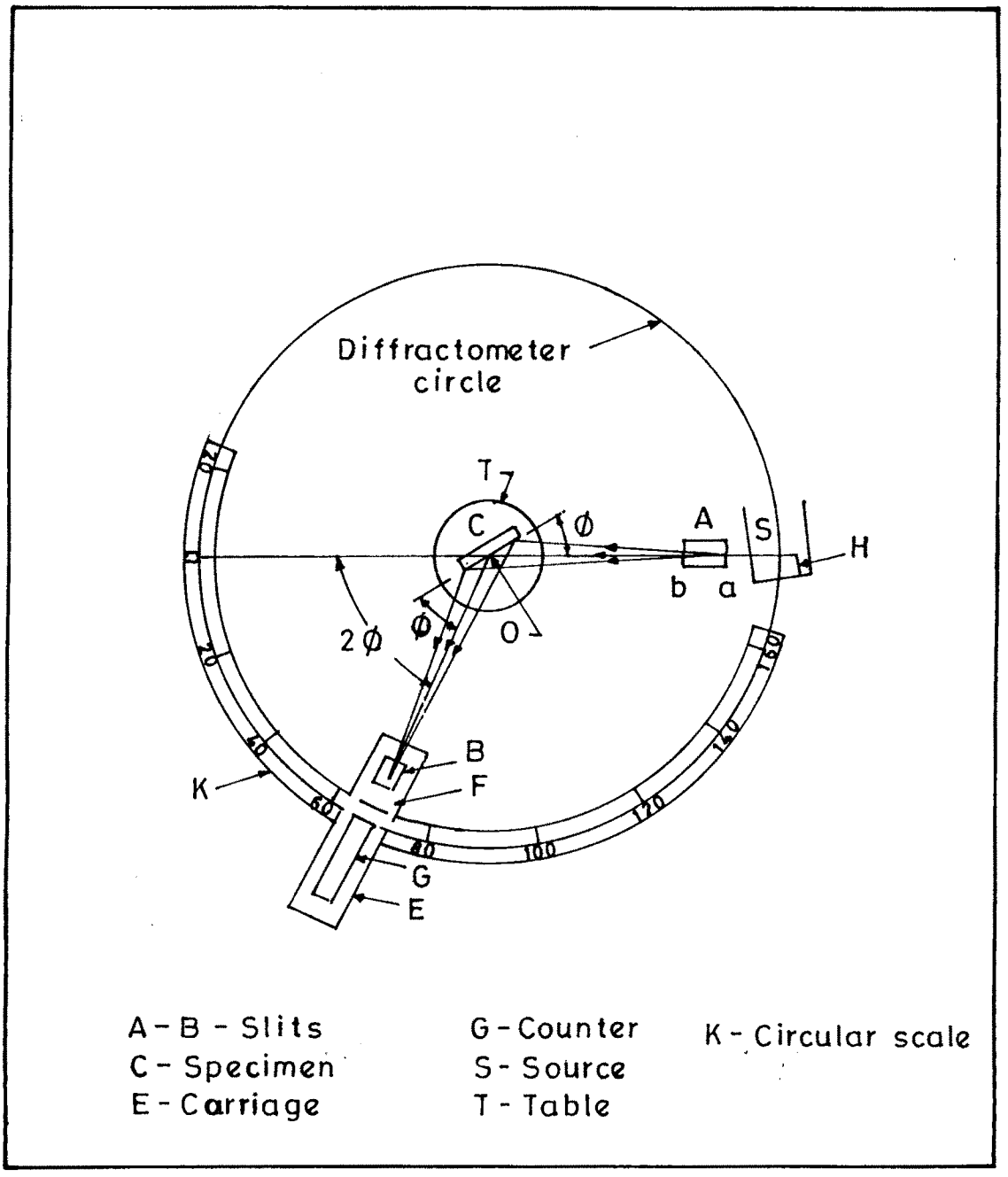

FIG. 3·1 - X-RAY DIFFRACTOMETER.

way that the rotation of counter through 2θ degrees is automatically accompained by rotation of the specimen through θ degrees. This coupling ensures that the angle of incidence and reflection from the specimen will always be equal to one another and equal to half the total angle of diffraction. The counter is set to such that the 2θ is nearly equal to zero and connected to counting -rate meter. The output of counting-rate meter is then fed to a strip chart - recorder. After this counter is driven at a constant angular velocity through increasing values of 2θ, so as to scan whole angular range. Simultaneouly the paper chart on the recorder moves at a constant speed, so that the distance along the length of the chart are proportional to 2θ. The resulting chart gives a record of counts per second (proportional to diffraction intensity) versus diffraction angle 2θ.

3.A.3 Experimental

The x-ray diffraction pattern of all the samples were record on Philips make x-ray powder diffractometer PW 1710 using Cuk_{α} radiation between 10 deg to 80 deg.

For cubic crystal structure interplaner distance(d), lattice parameter(a) and Miller indices (hkl) are related by the relation

$$d_{hkl} = \frac{a}{h^2+k^2+l^2} \qquad \text{.... 3.3}$$

For first order diffraction, Bragg's law

$$2d_{hkl} \sin\theta_{hkl} = \lambda \qquad \text{.... 3.4}$$

From equation 3.3, above equation becomes

$$(h^2+k^2+l^2) = \frac{4a^2\sin^2\theta}{\lambda^2} \qquad \text{.... 3.5}$$

The prominent line in the diffraction pattern of the spinel structure corresponds to (311) plane. With the help of this diffraction line and equation 3.3, lattice parameter 'a' can be calculated. Once the value of θ is known, it is possible to determine a set of integer $(h^2+k^2+l^2)$ and then indices of each plane.

The bond lengths for tetrahedral (A) and octahedral (B) sites can be calculated by using the equation [21].

$$A\text{-}O = (u\text{-}1/4)\, a\sqrt{3} \qquad \text{.... 3.6}$$

$$B\text{-}O = (5/8 - u)a \qquad \text{... 3.7}$$

Ionic radii on tetrahedral (A) and octahedral (B) sites for cubic samples were calculated by using the relation

$$R_A = (u\text{-}1/8)a\sqrt{3} - r_o^{2-} \qquad \text{.... 3.8}$$

$$R_B = (5/8\text{-}u)\, a - r_o^{2-} \qquad \text{.... 3.9}$$

where $r_o^{2-} = 1.35$ A°, radius of oxygen ion and u - oxygen ion parameter.

The x-ray density (ρ_x) and porosity(p) of the samples were calculated by the equations

$$\rho_x = \frac{8M}{Na^3} \qquad \text{.... 3.10}$$

$$p = \frac{\rho_x - \rho_s}{\rho_x}$$

$$p = \frac{\rho_x - \rho_s}{\rho_x} \times 100 \qquad \ldots 3.11$$

M - Molecular weight of the sample

N - Avagadrou's number

3.A.2 Results and discussion

The x-ray diffraction patterns revealed that the formation of single phase cubic spinels, showing well defined reflections of allowed planes without any impurity phase.

The x-ray diffraction patterns for the composition x=0, 0.20, 0.40, 0.60, 0.80 and 1.00 are presented in Figures 3.2 to 3.4. The interplaner distances 'd' were calculated using equation 3.3. The calculated and observed values of interplaner distances are in good agreement with each other. The lattice parameter was determined for the different compositions using the relation 3.5.

The plot of lattice constant versus zinc content shows linear variation as presented in Fig. 3.5. Similar behaviour is already reported by Daniel's, Rosenwaig [22] and Srivastava et al [23] for Ni-Zn ferrites system prepared by ceramic method. The increasing lattice constant with zinc concentration is due to the larger ionic radius of zinc (0.83 A^0), which on substitution replaces Fe^{3+} (0.67 A^0) ion from A site to B-site. The values of lattice constants in the present method are smaller than those of ceramic method. Similar conclusion was drawn by Takada et al [24]. The bond lengths and ionic radii on tetrahedral and octahedral sites have been calculated by using equations 3.6

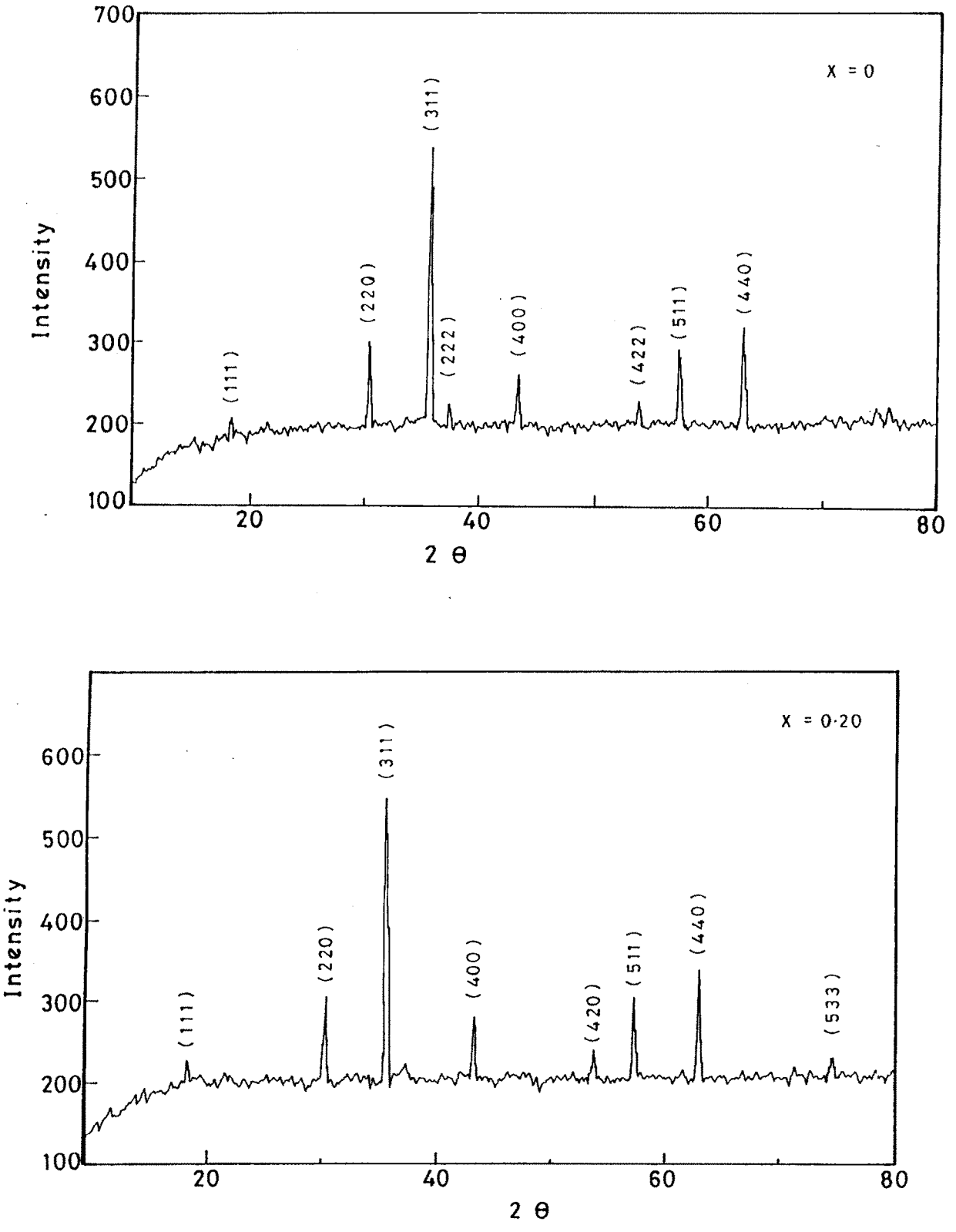

FIG. 3·2 – X-RAY DIFFRACTION PATTERN OF $Ni_{1-x}Zn_xFe_2O_4$ SYSTEM (X = 0 ; 0·20)

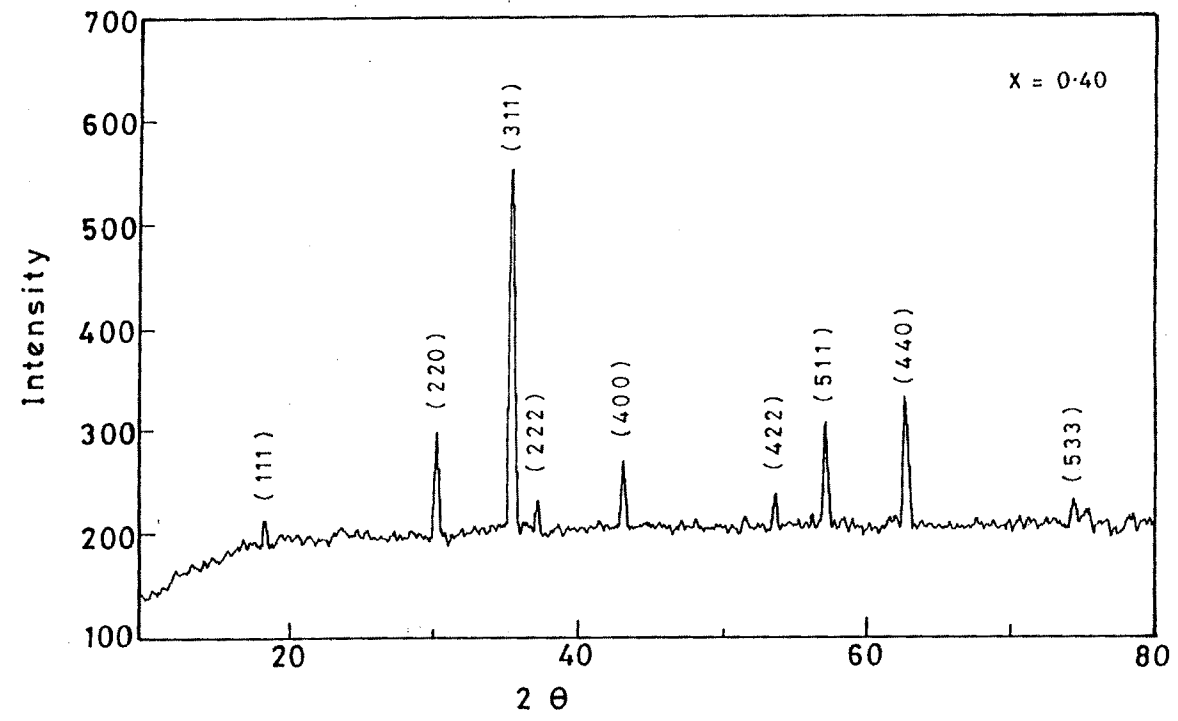

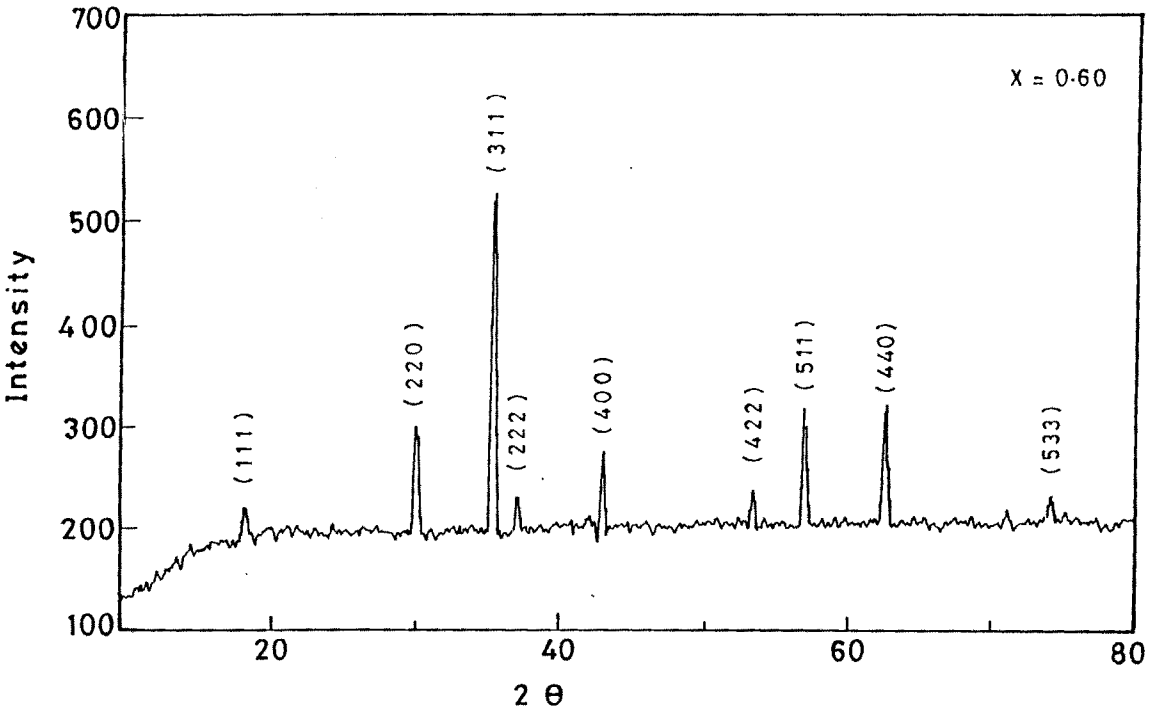

FIG. 3·3 - X-RAY DIFFRACTION PATTERN OF $Ni_{1-x}Zn_xFe_2O_4$ SYSTEM (X = 0·40 , 0·60) .

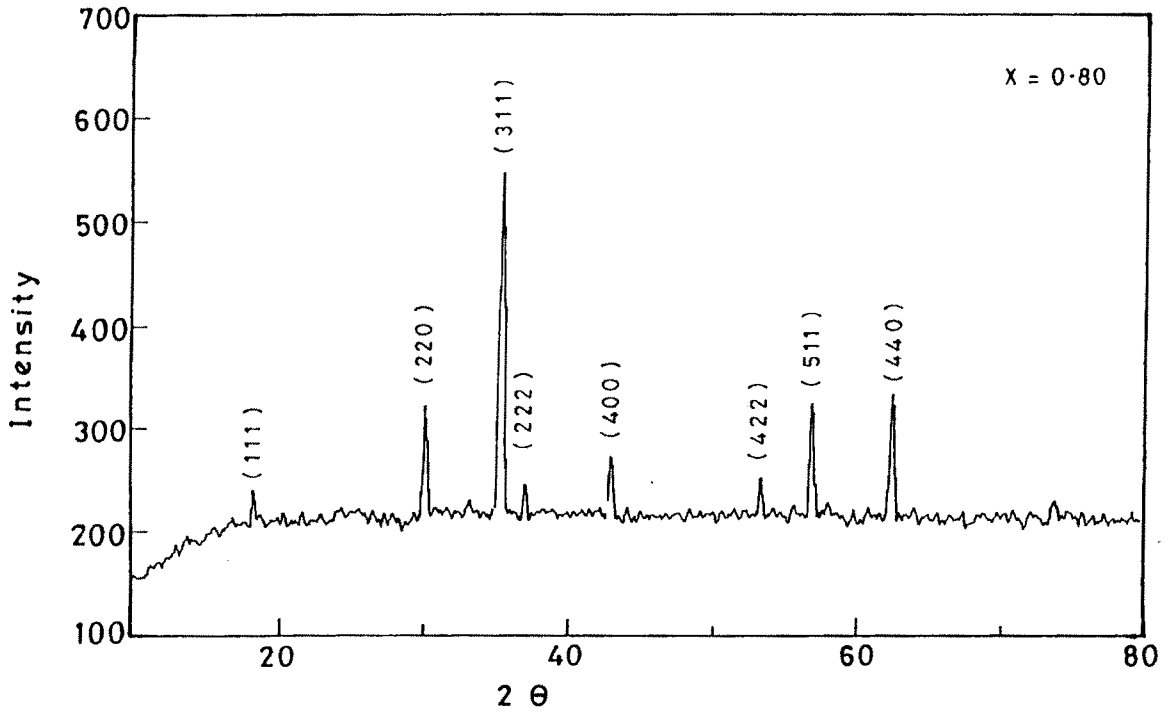

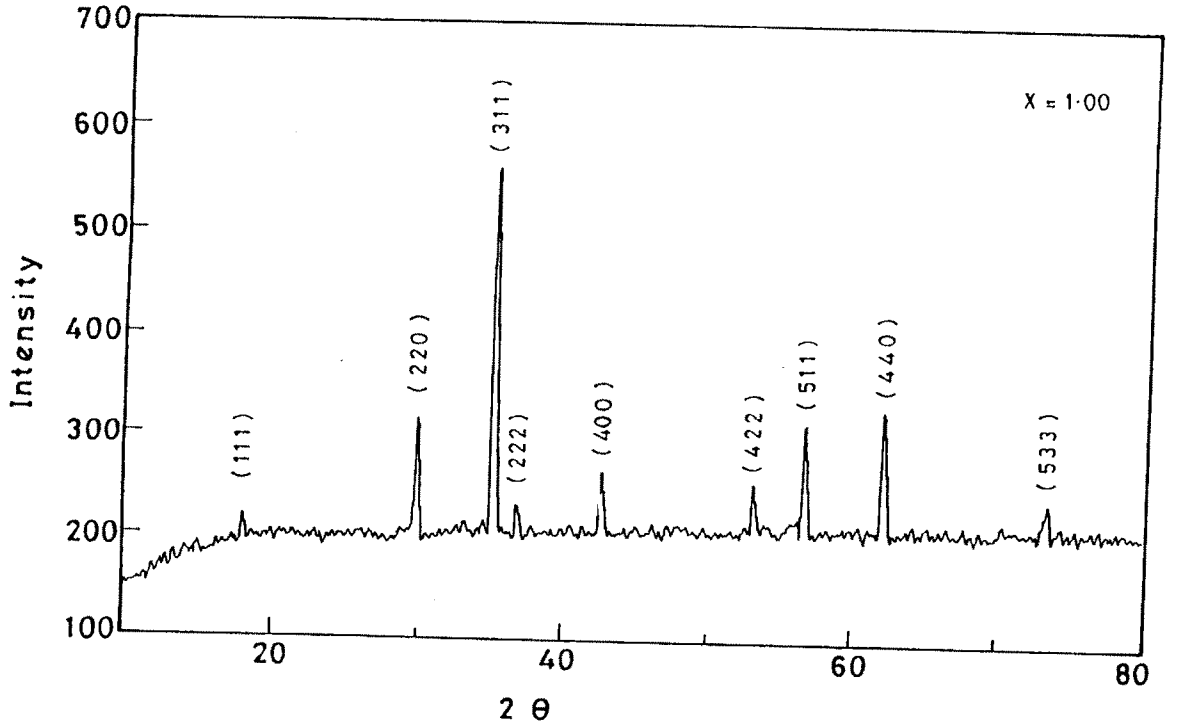

FIG. 3·4 - X-RAY DIFFRACTION PATTERN OF $Ni_{1-x}Zn_xFe_2O_4$ SYSTEM (X = 0·80 , 1·00)

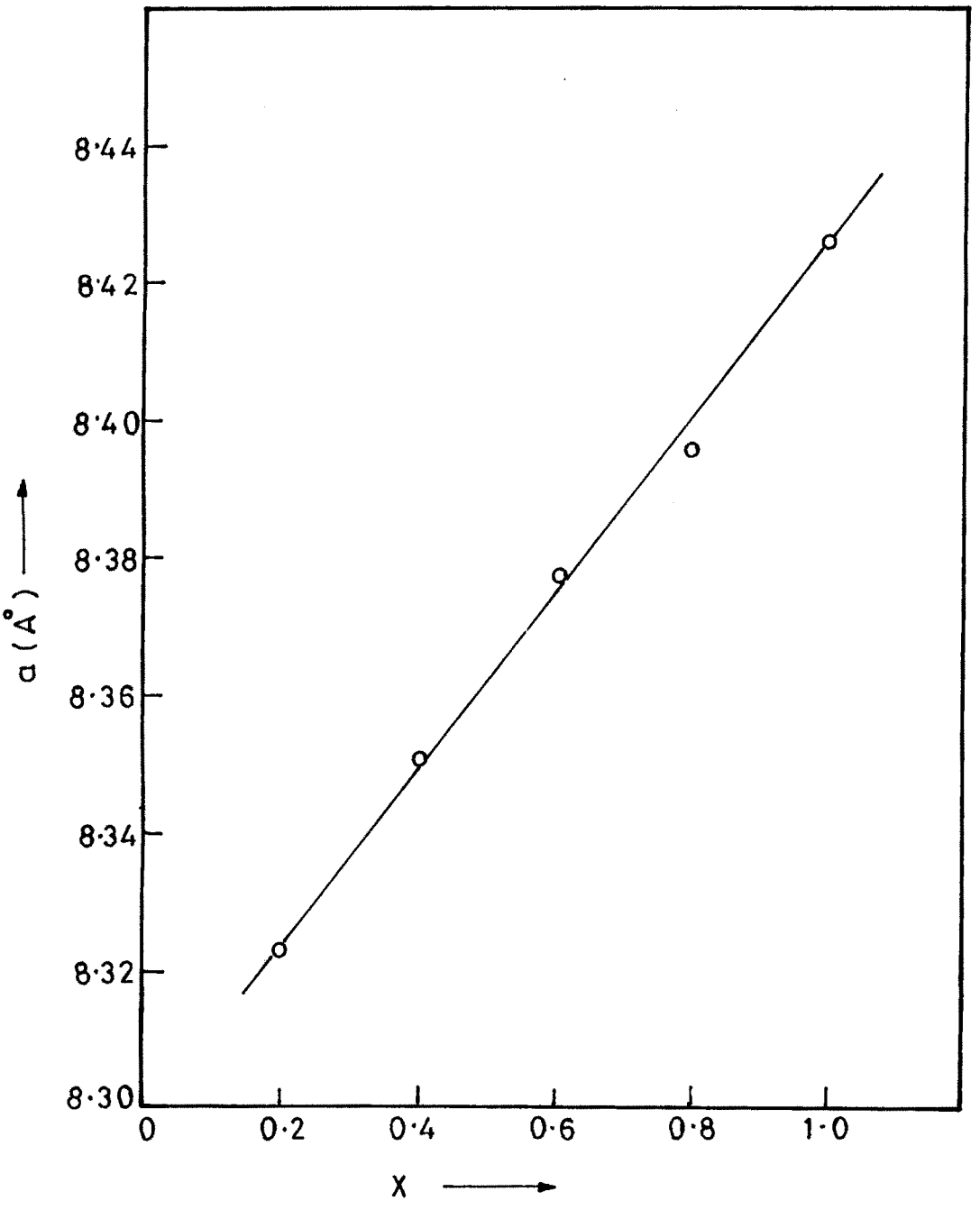

FIG. 3·5 - VARIATION OF LATTICE CONSTANT WITH ZINC CONCENTRATION.

to 3.9 and are presented in table 3.1. The values of oxygen parameters u used for the calculations are 0.381 A° for nickel ferrite and 0.385 A° for zinc ferrite. The average values were used for intermediate samples.

Table 3.1

X-ray diffraction data of $Ni_{1-x}Zn_xFe_2O_4$ system

Zinc content x	X-ray density ρ_x gm/cm^3	Lattice constant a A°	Bond lengths A°		Ionic radii A°	
			A-O	B-O	R_A	R_B
0	5.41	8.32	1.88	2.03	0.53	0.68
0.20	5.43	8.33	1.90	2.02	0.55	0.67
0.40	5.41	8.35	1.92	2.02	0.57	0.67
0.60	5.38	8.39	1.94	2.02	0.59	0.67
0.80	5.38	8.40	1.95	2.02	0.60	0.67
1.00	5.36	8.43	1.97	2.02	0.62	0.67

From the table 3.1, it is observed that radii on A site (R_A) increases with content of zinc. As can be seen from cation distribution [22], Zn^{2+} is occupying A sites therefore radii on A site will be increasing. The X-ray density was determined for different compositions using the relation 3.10 and presented in the same table.

Part B : IR Absorption

3.B.1 Experimental

Infrared spectra of six samples of $Ni_xZn_{1-x}Fe_2O_4$ (x=0.0, 0.20, 0.40, 0.60, 0.80 and 1.00) system were recorded on a Perkin-Elmer 783 IR spectrophotometer in the range of 200 - 800cm^{-1} at room temperature. The pellet used for recording the spectra were prepared by mixing small amount of ferrite powder in KBr.

3.B.2 Results and discussion

The IR spectrophotometer studies of the compositions support the formation of the spinel ferrites giving two absorption bands at 400 cm^{-1} and 600 cm^{-1} for octahedral and tetrahedral sites respectively.

The figures 3.6 to 3.8 shows the IR absorption spectras for the composition x= 0.0, 0.20, 0.40, 0.60 0.80 and 1.00. The value of absorption bands corresponding to higher and lower wave numbers are presented in table 3.2. The higher and lower absorption bands are seen to be around 600 cm^{-1} and 400 cm^{-1} respectively. Waldron [15] attributed the higher absorption band position (600 cm^{-1}) to the intrinsic vibrations of tetrahedral complexes and the lower absorption band position (400 cm^{-1}) to octahedral complexes, because of the difference in Fe^{3+} - O^{2-} distances for the octahedral and tetrahedral sites.

From table 3.2, it is observed that, wave number corresponding to tetrahedral vibrations goes on decreasing with increasing zinc content and is

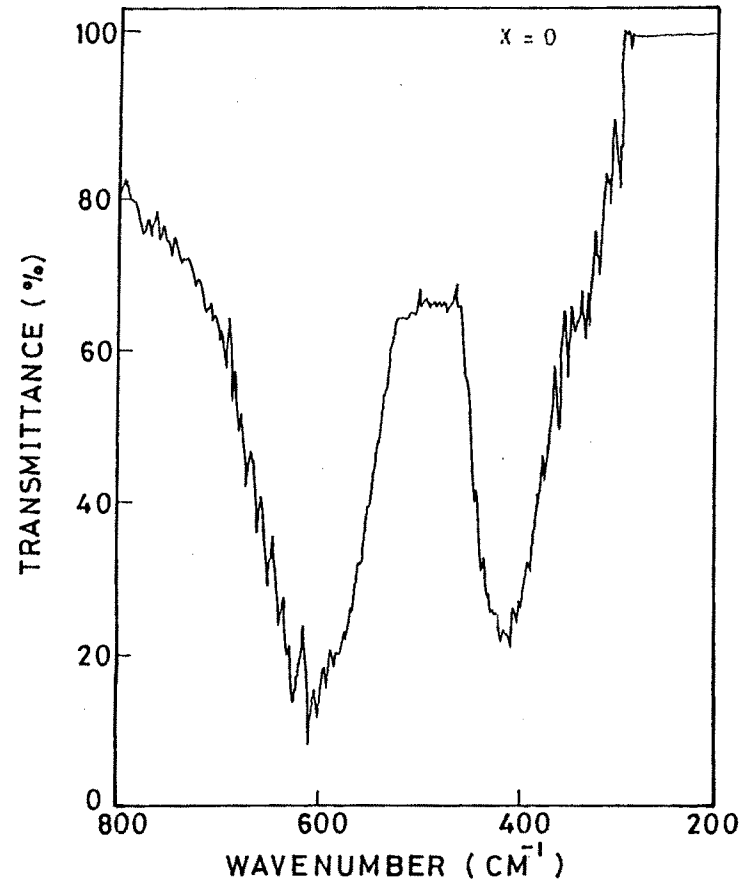

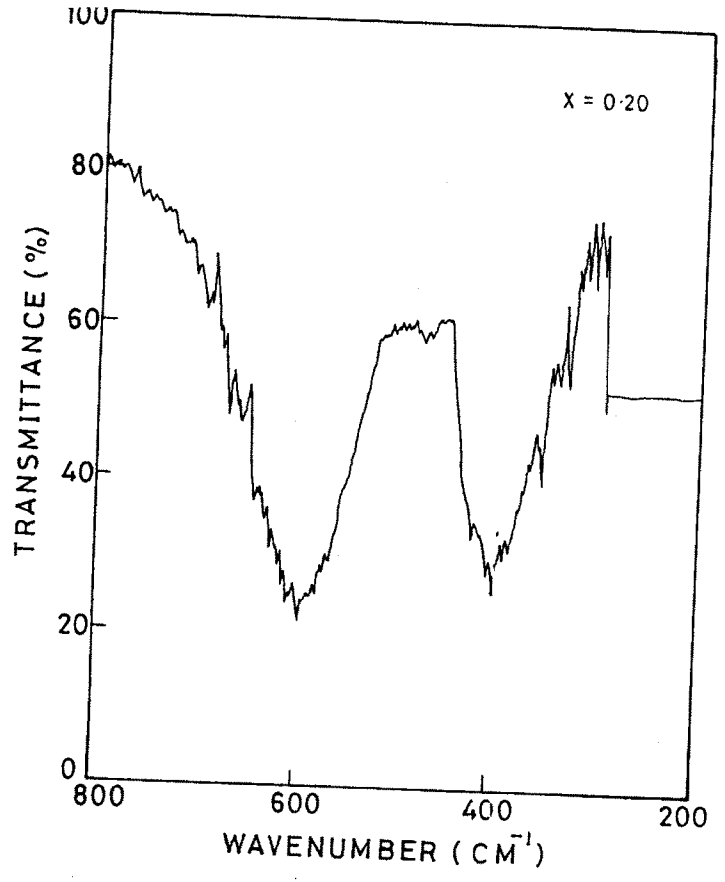

FIG. 3·6 – IR ABSORPTION SPECTRA OF $Ni_{1-x}Zn_xFe_2O_4$ SYSTEM (X = 0 , 0·20)

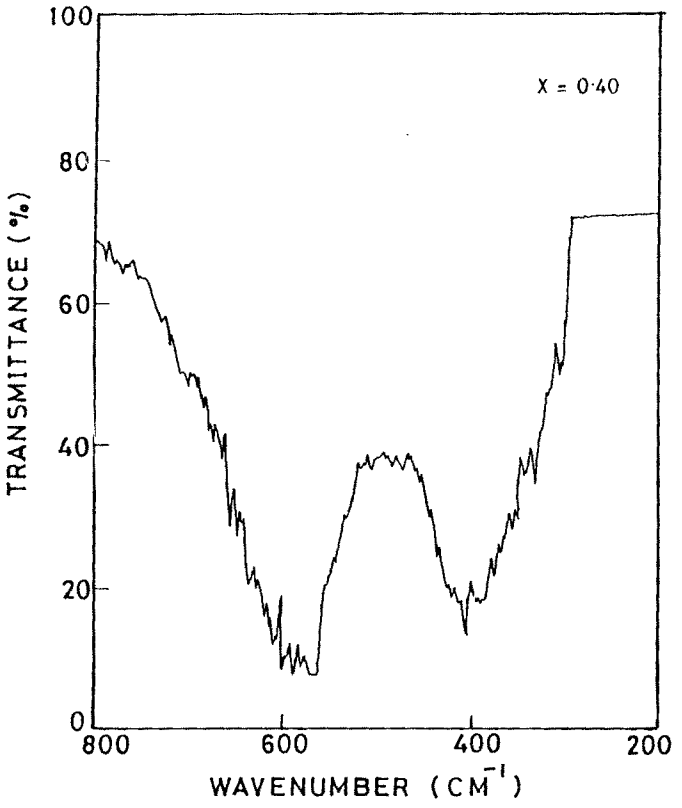

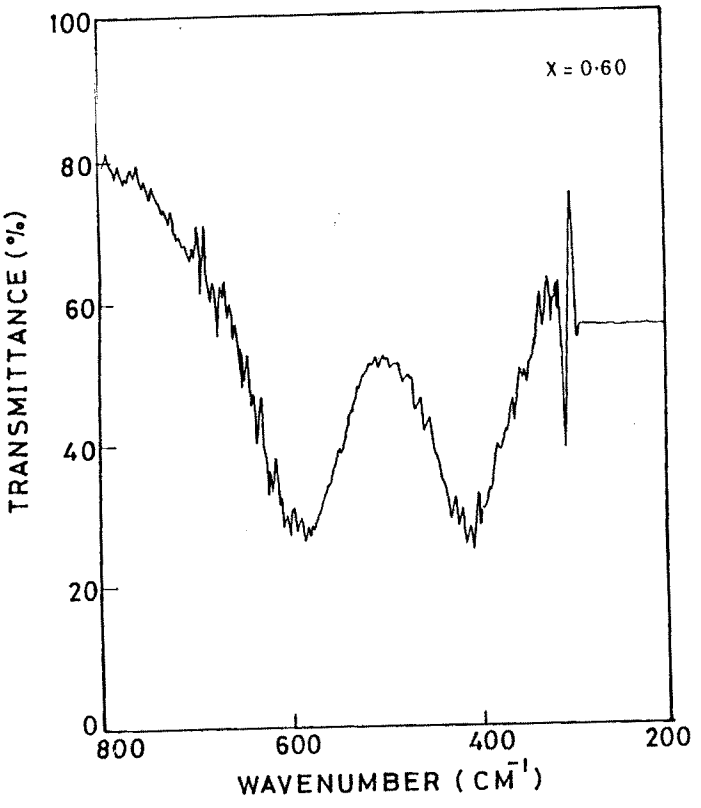

FIG. 3·7 - IR ABSORPTION SPECTRA OF $Ni_{1-x}Zn_xFe_2O_4$ SYSTEM (X = 0·40, 0·60)

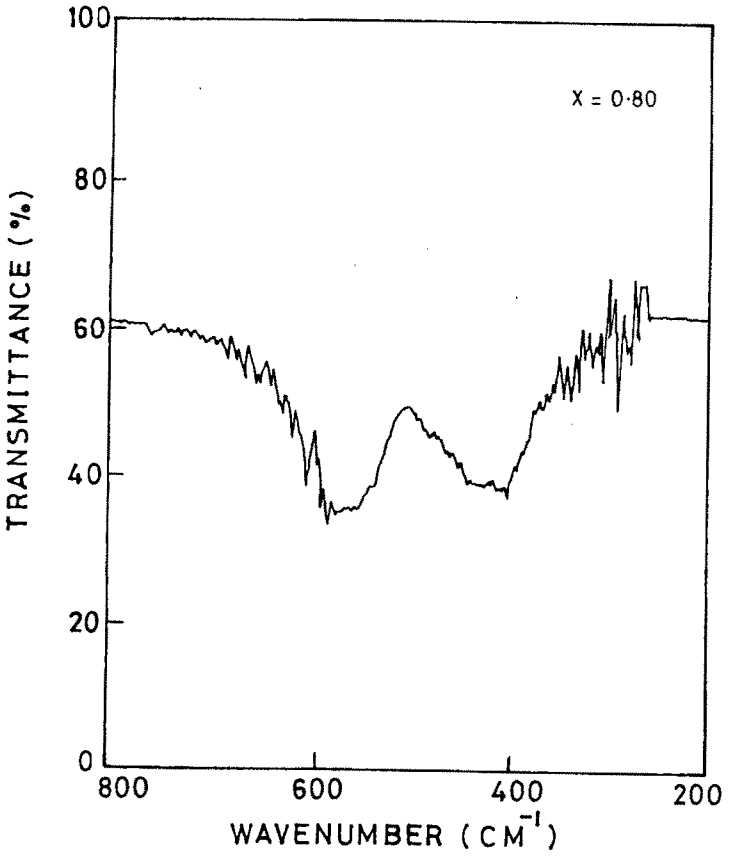

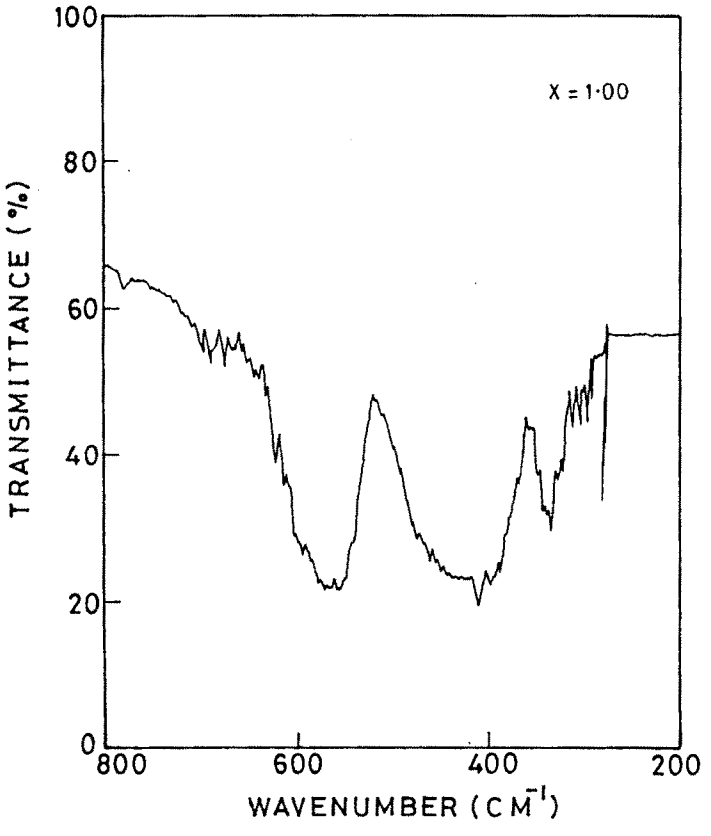

FIG. 3·8 – IR ABSORPTION SPECTRA OF $Ni_{1-x}Zn_xFe_2O_4$ SYSTEM (X = 0·80, 1·00)

minimum for $ZnFe_2O_4$. However there are no any remarkable changes observed in the position of wave numbers corresponding to octahedral vibrations. Potakova et al [18] also found the similar variation in wave numbers corresponding to tetrahedral vibrations for $Ni_{1-x-y}Fe_x^{2+}Zn_yFe_2^{3+}O_4$.

The IR absorption spectra of $ZnFe_2O_4$ presented in figure 3.8 shows an additional peak at about 330 cm^{-1} where as Srivastava and Srinivasan [25] observed an additional peak at about 338 cm^{-1} for zinc ferrite prepared by conventional ceramic method. This slight deviations of the position of bands are mainly due to the factors like method of preparation, grain size and density [26].

With the help of molecular weights of cations on A and B sites and absorption wave numbers ν_1 and ν_2, the force constants were calculated by using Waldron analysis and are given in Table 3.2.

From this table, it is observed that force constants on tetrahedral site (K_t) shows decreasing trend while force constants on octahedral site (K_o) shows increasing trend with increasing zinc concentration. Similar variations in K_o, and K_t were observed by Waldron [15] in nickel and nickel -zinc ferrites.

Tabel 3.2

IR absorption data of $Ni_{1-x}Zn_xFe_2O_4$ system

Zinc content x	Absorption bands cm^{-1}			Force constants dyne/cm	
	ν_1	ν_2	ν_3	$K_t \times 10^5$	$K_o \times 10^5$
0	604	403	-	2.17	1.28
0.20	594	405	-	2.16	1.30
0.40	589	403	-	2.11	1.31
0.60	582	404	-	2.07	1.32
0.80	587	407	-	2.16	1.32
1.00	552	405	330	1.93	1.29

References

1. Bragg W.L., Nature, (London), 95 (1915) 561.
2. Bertaut M.F., Compt. Rand., 228 (1949) 492.
3. Waren B.E. and Aberbach B.L., J. Applied Phys., 21 (1950) 595.
4. Bhosale D. N., Chaudhari N.D., Shashiknat R. Sawant, R.D. Kale and P.P. Bakare, IEEE, Trans. On Mag., 34 (2) (1998) 535.
5. Pandya H.N and Kulkarni R.G., Solid State communications , 61 (10) 1987 645.
6. Karche B. R., Khasbardar B.V., and A.S. Vaingankar, Journal of Magnetisum and Magnetic Materials, 168 (1997) 292.
7. Baijal J.S., Kothan D., and Phajoubam, Proc. ICF -5, India (1989) 371.
8. Dorik R. G., Kunal B., Modi and Jadhav K.M., Ind. J. of Pure and Applied phys., 23 (1997) 594.
9. Patil M.G., Mahajan V.C, Ghatage A.K., and Patil S.A., Ind. J. of Pure and Applied physics, 34 (1996) 166.
10. Vasambekar P.N., Kolekar C.B., and Vaingankar A.S, Material Research Bulletin., 34 (6) (1999) 863.
11. Ravidranatahn P, and Patil K.C., J. of Mat. Science, 27 (1987) 3261.
12. Yamaura H., Kakio T., Haneda H., Watanabe A. and Shiraski, Yogyo-Kyokai-Shi (Japan) 94 (4) (1986) 393
13. Kulkarni R.G. and Joshi H.H., J. Solid State Chem., 64 (1986) 141.

14. Kendall D.N., "Applied infrared spectroscopy", Reinhold Publishing Corp., Chapman and Hall Ltd. London (1966)1.

15. Waldron R.D., Physical Review Volume 9 (6) (1955) 1727.

16. Josyulu O.S., and Sobhanadri J., Phys. Stat. Solution, (a) 65 (1981) 65.

17. Reddy P.V. and Salagram M., Phys. Sta. Soln., (a) 100 (1987) 639.

18. Potakova V.A, Zerery W.D. and Romancv V.R., Phys. Stat. Soln. (a) 12 (1972) 623.

19. Debye P. and Scherrier P., Physics, 17 (1916) 277 and 18 (1977) 219.

20. Hull A.N., Phys. Rev., 9 (1916) and 10 (1917) 661.

21. Smith J. and Winj. H.P.J., "Ferrites" Physical properties of ferrimagnetic oxides in relation to their technical application, Philips. Tech. Library, (1959).

22. Daniels J.M. and Rasenewaig A., Canadian Journal of Physics, 48 (1970) 381.

23. Srivastava C.M., Shringi S. N., Patani M.J., and Joglekar S.M., Bull. Mater. Sci., 6 (1) (1984) 1.

24. Toshio Takada, Yashichika Banbo, and Teruya Shwjo, Proc. IC, Japan (1970) 29.

25. Srivastava C.M., and Srinivasan. T.J., J. App. Phys.., 53 (1982) 8148.

26. Murthy S.R, Citra Sankar S., Reddy K.V., and Sobahanadri J., Ind. J. of Pure and Applied Physics., 16 (1978) 79.